

# Design a remote sensing of multi-BOTDR fiber optic sensors for fuel pipeline monitoring

Arafat A. A. Shabaneh, Raed S. M. Daraghma

Department of Telecommunication Technology Engineering, Faculty of Engineering and Technology,  
Palestine Technical University–Kadoorie (PTUK), Tulkarm, Palestine

---

## Article Info

### Article history:

Received Aug 07, 2021

Revised Oct 21, 2022

Accepted Nov 02, 2022

---

### Keywords:

Bidirectional optical fiber

Brillouin scattering

Remote sensing

Scattering threshold power

---

## ABSTRACT

The necessity for environmental protection has led to the development of different sensors for monitoring fuel pipelines to avoid explosion, leakage, and corrosion. Distributed optical fiber sensors-based Brillouin scattering have become progressively common because of their novel feature of simultaneously determining temperature, vibration, and strain. The stimulated Brillouin scattering (SBS) threshold power, sensing distance, single-mode fiber cable length, and sensing accuracy are serious parameters to the implementation of Brillouin optical time-domain reflectometry (BOTDR) sensor. In this study, remote sensing of multi-BOTDR fiber optic sensors for fuel pipeline monitoring is designed and presented. The results of simulations and theoretical explanations on suppressing fiber optic nonlinearity are analyzed. Results show that an SBS suppression via 16 dB is required to attain the maximum multi-remote sensing distance of up to 20 km for each network and a perfect frequency shift of 11 GHz. An open eye pattern corresponds to minimal signal distortion with a high Q-factor of 22 for the developed sensor. The highest sensing accuracy of 0.3318 %/K indicating power change (%) is observed from 290–300 K at 193.1 THz operating frequency.

*This is an open access article under the [CC BY-SA](https://creativecommons.org/licenses/by-sa/4.0/) license.*



---

## Corresponding Author:

Arafat A. A. Shabaneh

Department of Telecommunication Technology Engineering, Faculty of Engineering and Technology

Palestine Technical University–Kadoorie (PTUK), Tulkarm, Palestine

Email: a.shabaneh@ptuk.edu.ps

---

## 1. INTRODUCTION

Monitoring fuel pipeline is a pressing issue in aspects of economy and security [1]. An early warning is sent via sensors to avoid explosion, leakage, and corrosion in pipeline networks [2], [3]. The monitoring process is automated, reducing inspection costs and decreasing catastrophic incidents. However, the length of fuel pipelines is exceeding hundreds of kilometers [4]. Therefore, optical fiber sensor has high evaluation performance in terms of accuracy, resolution, and backscattered power level [5]. Backscattered signals are weak in the Brillouin scattering mechanism, reducing the nonlinear effects that lead to retrogression of the sensor performance. Many methods are suggested to raise the threshold power of stimulated Brillouin scattering (SBS) [6]. A low SBS threshold power requires a high input power level to be launched into the sensor to obtain a high backscattered power level exclusive of nonlinear effect. In turn, SBS will decrease the accuracy and the maximum range of the sensor. Former suppression performances have focused on a single suppression method depending on experience and theoretical discussion. Nevertheless, factors, such as increasing the SBS threshold power, maximizing the sensing distance, suppressing fiber nonlinearity, and enhancing the sensor resolution, affect the SBS threshold [2], [7]-[9].

Distributed optical fiber sensor techniques are usually based Brillouin optical time-domain reflectometry (BOTDR). Light scattering can be measured by BOTDR but requires high sensitivity and classified into linear scattering (Rayleigh and Mie) and nonlinear scattering (Brillouin and Raman). Moreover, Brillouin scattering can be categorized as spontaneous Brillouin scattering and stimulated Brillouin scattering [10]-[12]. Brillouin scattering is temperature sensitive and occurs due to the thermally excited acoustic vibrations produced via light beam propagation along with the optic fiber [13]. A phonon of acoustic frequency and a scattered photon are created via incident photon in Brillouin scattering operation. This phenomenon forms a frequency shift (zero in the forward direction and maximum in the backward direction) sensitive to temperature variation [14].

BOTDR utilizes spontaneous Brillouin scattering. Spontaneous Brillouin backscattering-based optical fiber sensors are investigated in several works [12], [15]. Yan and Chyan [2] designed an improved BOTDR fiber optic sensor system for oil as well as gas pipeline monitoring. They applied spontaneous Brillouin backscattering-based fiber optic sensors to study theoretical and experimental works in temperature sensing applications. They obtained a Brillouin backscattered power coefficient  $P_B$  of 0.332 %/K and regarded an SBS suppression of 11 dB as a requirement to obtain the maximum sensing distance. The current project aims to employ spontaneous Brillouin scattering-based fiber optic as remote sensing for pipeline monitoring to design and simulate remote sensing of multi-BOTDR sensors on the basis of spontaneous Brillouin scattering mechanism. The Optisystem software is used to model the design accurately and increase the SBS threshold power toward the maximum sensing distance.

## 2. SIMULATION DETAILS AND PRINCIPLE

### 2.1. Bidirectional optical fiber

Factories have a complicated construction and an association of facilities within a huge place. Consequently, the throughput decreases or accidents arise unless the facilities are accurately maintained and managed. This study proposes a solution to enhance productivity via efficiently gathering temperature, vibration, and strain data by installing fiber optic sensors in factory facilities, as shown in Figure 1. The developed design analyzes the signals to improve health, security, environmental friendliness, and maintainability.

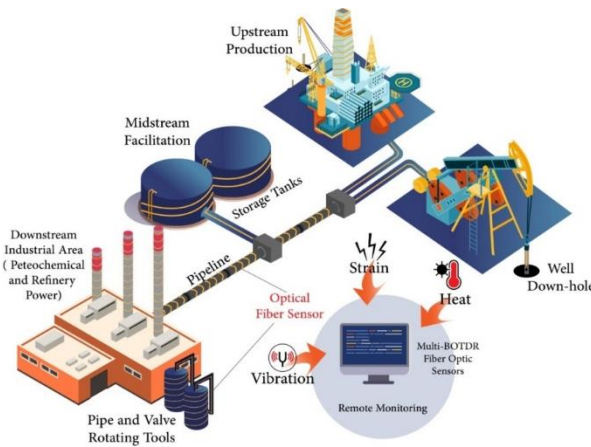


Figure 1. Applications of optical fiber sensors for factories

Rayleigh scattering (RS) is the dominant intrinsic loss appliance in the low-absorption window between the ultraviolet as well as infrared absorption tails. RS fallouts from inhomogeneities of a random nature happening on a tiny scale compared with the light wavelength. The RS formula is given by [16], [17].

$$\gamma_R = 8\pi^3/3\lambda^4 (n^8 p^2 \beta_c K T_F) \quad (1)$$

Where  $\gamma_R$  is the RS coefficient.  $\lambda$  is the optical wavelength,  $n$  is the refractive index (RI) of the medium,  $p$  is the average photoelastic coefficient,  $\beta_c$  is the isothermal compressibility at a fictive temperature  $T_F$ , and  $K$  is Boltzmann's constant. The RS coefficient is related to the fiber transmission loss factor which calculated by [16], [17].

$$L = \exp(-\gamma_R l) \quad (2)$$

Where  $l$  is the fiber length.

The backscattered light spectrum peaks composed of Rayleigh, Brillouin, and Raman scattering are shown in Figure 2. A relationship exists between the wavelength and the intensity of scattering, and the Brillouin scattering (red peak) depends on the temperature and strain. Within the fiber, SBS is the modulation of light during thermal molecular vibrations. Through the modulation frequency, scattered light performs as upper and lower sidebands detached from the incident light.

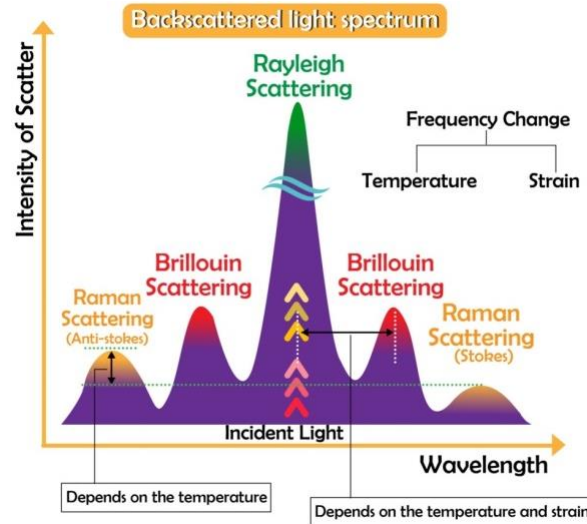


Figure 2. Backscattered light spectrum

In the scattering operation, the incident photon generates a phonon of acoustic frequency and a scattered photon. This phenomenon yields an optical frequency shift, which changes with the scattering angle given that the sound wave frequency changes with acoustic wavelength. The frequency shift is maximum in the backward direction and decreases to zero in the forward direction, making SBS a chiefly backward operation. The threshold optical power  $P_{SBS}$  is given by [16], [18], [19].

$$P_{SBS} = 4.4 \times 10^{-3} d^2 \lambda^2 \alpha_{dB} \nu \text{ watts} \quad (3)$$

Where  $d$  is the fiber core diameter ( $\mu\text{m}$ ),  $\lambda$  is the operating wavelength ( $\mu\text{m}$ ),  $\alpha_{dB}$  is the fiber attenuation in dB/km, and  $\nu$  is the source bandwidth (GHz).

In other words,  $P_{SBS}$  is the input power where the backscattered power is equivalent to the transmitted power. The SBS threshold may be calculated approximately by applying the (4) [2], [18].

$$P_{SBS} \cong 21 (KA_{eff}/g_B L_{eff}) \quad (4)$$

Where  $P_{SBS}$  is the SBS threshold power.  $K$  is the polarization factor, and  $A_{eff}$  is the effective core area of the sensing fiber.  $g_B$  is the Brillouin gain constant.  $L_{eff}$  is the effective length defined via a fiber attenuation coefficient, and  $\alpha$  besides length  $L$  are given by the following relation [2], [18].

$$L_{eff} = (1 - e^{-\alpha L})/\alpha \quad (5)$$

Where  $\alpha$  is the attenuation coefficient of the fiber, while  $L$  is the fiber length.

The Brillouin frequency shift relies on the temperature, as shown in the distributed temperature sensor, which is linearly proportional. Differences are also observed in the RI of the fiber. The Brillouin frequency is expressed as [4].

$$V_B(T) = V_{B0} + dV_B/d_T(T - T_0) \quad (6)$$

Where  $V_{B0}$  is the Brillouin frequency at a reference temperature  $T_0$ , moreover [4]:

$$V_B = 2nV_A/\lambda \quad (7)$$

Where  $n$  is the RI,  $V_A$  is the acoustic velocity, and  $\lambda$  is the incident light wavelength.

Bidirectional optical fiber is affected and sensitive to various factors, such as temperature, vibration, and strain. The principal operation of the BOTDR sensor is shown in Figure 3. The incident light (purple arrow) passes in the core along the bidirectional optical fiber to be transmitted, whereas some of the light is scattered (yellow arrow) and backscattered (green arrow). The backscattered light is detected by an optical power meter and optical spectrum analyzer. These instruments are used to measure the SBS threshold power and investigate the frequency shift, respectively. The (8) can be used to calculate the distance  $z$  (black arrow), as shown in Figure 3.

$$z = tV/2 \quad (8)$$

Where  $t$  is the two-way propagation delay time, and  $V$  is the velocity of light in the fiber.

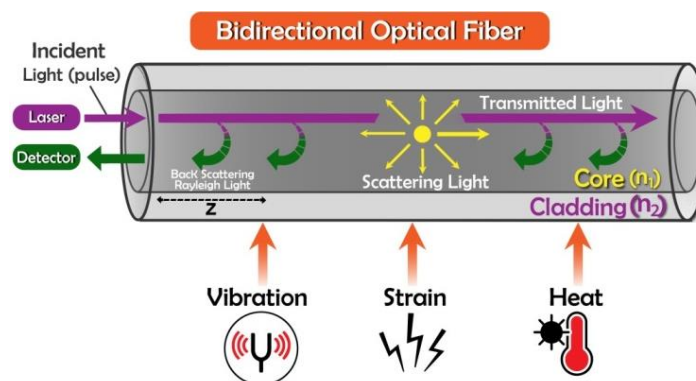


Figure 3. Principle of the bidirectional optical fiber

## 2.2. Component description

A pseudo-random bit sequence generator is applied to produce a continuous random data signal in bit rates. The operation process is organized via an algorithm to generate the bit sequence of zeros and ones. The modulation process needs an electrical data signal generated via a non-return-to-zero (NRZ) pulse generator. NRZ determines the bits in a specific state as the voltage changes. Thus, specifying where the bits must start and stop should be easy. The rise and fall times for the laser signal are equal to 0.05 bit. In addition, one of the advantages of the NRZ pulse generator lies in its bandwidth control. Consequently, the returning signals to zero between bits do not waste the bandwidth of the data signal [20], [21].

A continuous-wave (CW) laser diode is applied to yield an optical signal that delivers an input signal with 1552.52 nm wavelength, 193.1 THz frequency, 10 MHz linewidth, and 0–32 dBm input power [22], [23]. A CW laser is connected with an NRZ pulse generator through an electroabsorption modulator (EAM) with a modulation index of 99%. EAM is an external optical modulator comprising two inputs (optical and electrical signals) and one output (optical). This component is the preferred candidate for telecommunication use considering zero biasing voltage, small driving voltage, low/negative chirp, small size, high speed, low polarization dependence, and integration with distributed feedback laser. Additionally, EAM provides a single optical power source for numerous data-carrying beams. EAM is a semiconductor device utilized for modulating the intensity of a laser beam through an electric voltage [24]. The operation fundamental of EAM is depending on the Franz–Keldysh effect. The applied electric field alters the absorption spectrum, directly changing the bandgap energy. Consequently, an electro-absorption modulator (EMA) modulator is suitable for prolonged distance transmissions of high-speed schemes [25].

A single-mode fiber (SMF) comprises a core with a small radius with high RI, and the cladding material has a low RI. The core permits the propagation of light in one mode enclosed by transparent cladding material. The light passing at the core follows the total internal reflection mechanism. SMF is also suitable for prolonged distance communications and computer networking transmissions with high-speed data rates and less attenuation compared with electrical transmission lines. The optical fiber cable length for the data signal transmission ranges from 25–100 km [20].

The optical fiber splitter component facilitates sharing in serving users, which can maximize the performance of optical network circuits. The fork 1×2 ports are applied to divide an incident light beam from a single input fiber cable into two light beams and transmit them over two individual output fiber cables. Each output line is connected with a bidirectional optical fiber of 10 km length as a separated monitoring network system. Bidirectional optical fibers are used as sensors based on the BOTDR mechanism.

Avalanche photodetector (APD photodiode) is a suitable receiver for long-haul communications. APD has many features, such as high gain, high signal-to-noise ratio, highly sensitive network access, and a tolerable and high-speed receiver in high bandwidth applications and bit rates [26]. Moreover, the APD photodiode has a responsivity of 1 A/W and a dark current of 10 nA. APD converts the optical signal into electrical output signals. These electrical signals are filtered through a low-pass Bessel filter, which reduces the noise and distortion without introducing a considerable amount of inter-symbol interference. The filter approximates are Gaussian-type filters. These filters aim to smoothen and sharpen the magnitude response. An insertion loss of 0 dB and a depth of 100 dB are considered for the developed design [20], [21]. The optical power meter and optical spectrum analyzer are connected to measure the total power (transmitted, Brillouin backscatter, and Rayleigh backscatter (RBS) power) and monitor the output signals (frequency shift), respectively. The eye diagram and bit error rate (BER) analyzers are used in the proposed design to measure and check the Q-factor, eye height, and minimum BER.

### 2.3. Simulation model and design consideration

A systematic block scheme of remote sensing of the multi-BOTDR fiber optic sensor and SMF for fuel pipeline monitoring is constructed. The simulation model designed in the Optisystem software is shown in Figure 4. The NRZ pseudo-random binary sequence generates the input signal, which contains electrical data represented by zeros as well as ones. Subsequently, the input signal is modulated with a semiconductor laser characterized by CW laser through the EMA modulator. The light from the CW laser source is modulated by intensity modulation, coupled into an SMF cable of 10 km, and linked to two bidirectional optical fibers.

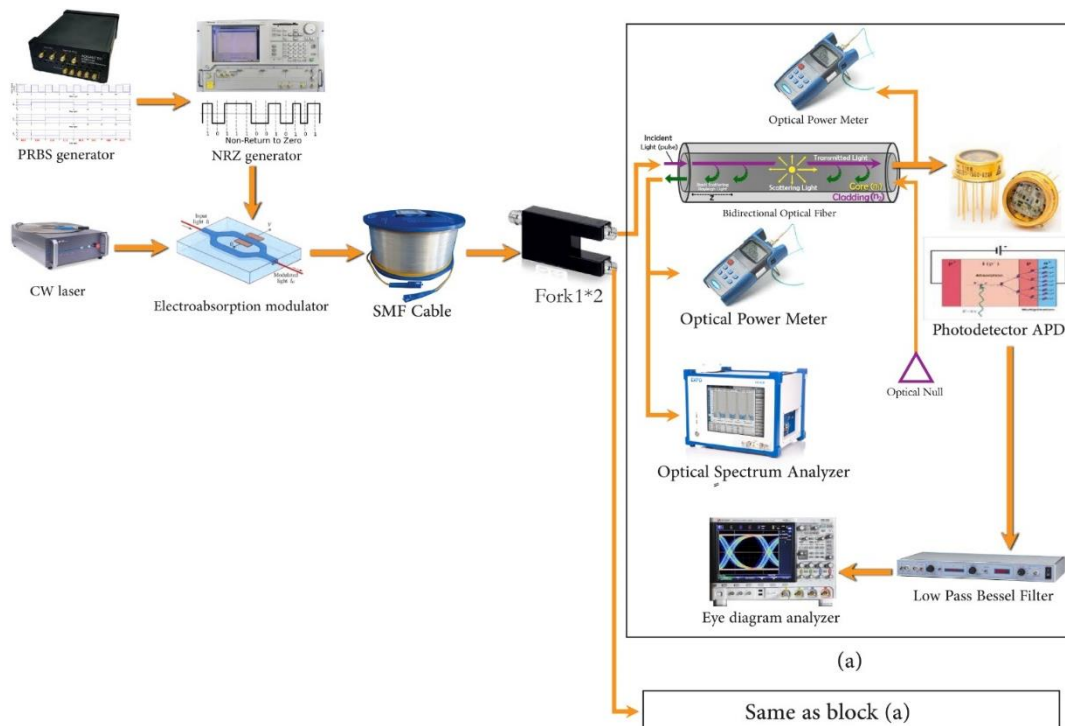


Figure 4. Simulation model design

The developed model comprises the CW laser source, EAM, SMF cable, fork 1×2, optical null, a receiver, and bidirectional optical fiber. In a bidirectional optical fiber, a collection of the scattered signal is observed. The receiver detects the transmitted and the Brillouin backscattered signal. Optical null is applied to terminate the bidirectional optical fiber connection. SMF is used with a bidirectional optical fiber. SMF has a high data rate and low dispersion and is appropriate for long-haul distances, making it adequate for remote sensing applications. The settings of the global simulation parameters chosen for the simulation model are shown in Table 1.

Bidirectional optical fibers are applied as a spontaneous Brillouin scattering for BOTDR sensors with SMF cable. The global simulation parameters selected for bidirectional optical fibers are shown in Table 2. The SBS threshold power  $P_{SBS}$  depends on the optimized parameters listed in Table 2.

Table 1. Simulation parameter settings

Parameters	Values
SMF length (km)	10
Attenuation index (dB/km)	0.5
Dispersion (ps/km/nm)	16.75
Dispersion slope (ps/nm <sup>2</sup> /km)	0.075
Reference wavelength (nm)	1552.52
Differential group delay (ps/km)	0.2
C/W input power (dBm)	0 to 32
Frequency (THz)	193.1

Table 2. Simulation parameter settings for the bidirectional optical fiber

Parameters	Values
Reference wavelength (nm)	1552.52
Attenuation (dB/km)	0.5
Effective area (μm <sup>2</sup> )	100
Polarization factor	2
Temperature (K)	300
Brillouin gain constant (m/W)	3e <sup>-011</sup>
Brillouin linewidth (MHz)	31.7
Rayleigh backscattering (1/km)	5e <sup>-005</sup>
Length (km)	10

### 3. RESULTS AND DISCUSSION

The sensor based on spontaneous Brillouin scattering was developed with a length of 10 km and a temperature of 300 K. The simulation and investigation of the layout were performed using the OptiSystem simulator 7.0 software. The schematic of remote sensing of the multi-BOTDR fiber optic sensor setup used for monitoring gas as well as oil pipeline is shown in Figure 5. The novelty of the developed simulation design was the multi-BOTDR fiber optic sensor application, resulting in high performance and ideal evaluation in the SBS threshold power and frequency shift. The SBS threshold power (dBm), eye diagram, frequency shift (Hz), minimum BER (dB), and Q-factor were tested and obtained for different values of optical input power and a fixed SMF length of 10 km with an attenuation coefficient of 0.5 dB/km.

At the bidirectional optical fiber port terminals, the optical power meters and optical spectrum analyzers were connected at the input and the output ports to measure the transmitted power, backscattered power, and frequency shift. Afterward, the optical signal was converted to an electrical signal via APD photodetector. The link performances of minimum BER and Q-factor were assessed by 3R-regenerator connected to eye diagram analyzers.

NRZ pulses are binary code wherein ones are denoted by a positive voltage, whereas zeros are denoted by a negative voltage, with no rest condition. Figure 6(a) demonstrates the binary signal of NRZ pulses. Besides, Figure 6(b) shows eye diagram of generated NRZ at the transmitter side.

The backscattered frequency in THz is shown in Figure 7. It was compared with the source frequency, where the propagated signal was 193.1 THz, and the backscattered frequency was 193.089 THz as shown in Figure 7. Accordingly, the frequency shift was 193.1 THz – 193.089 THz = 11 GHz. The Brillouin frequency shift was 11 GHz. The simulation result accurately revealed the effect of Brillouin scattering on frequency shift and power level [2], [4].

The eye diagram with minimum BER is presented in Figure 8. The eye diagram is clear and open, and the waveform distortion is substantially reduced with a high value of Q-factor at 0.5 dB/km attenuation for 10 km length as demonstrated in Figure 8. Open and clear eye diagrams with low BER are achieved. This finding implies enhanced performance of the system and corresponds to minimal signal distortion. The results reveal that the eye-opening decreases with the increase in transmitted power. Consequently, the signal depletes when the input power increases. The red line represents the curve of the minimum BER for the developed design. At an SBS threshold power of 16 dBm, the developed design offers reduced signal distortion and improved eye opening with 22 Q-Factor, and the minimum BER was 6.27719e<sup>-108</sup>.

The developed design successfully constructed a set of improved settings that could suppress the SBS threshold power. Beside a high SBS threshold power, the sensing distance could be prolonged. The SBS threshold power was 16 dBm for the sensor after parameter optimization of the SBS suppression for the bidirectional optical fiber, as displayed in Figure 9. The input power was 0–32 dBm, which was applied to run simulations to obtain the SBS power threshold point. A step of 1 dBm resulted in a change in the input power.

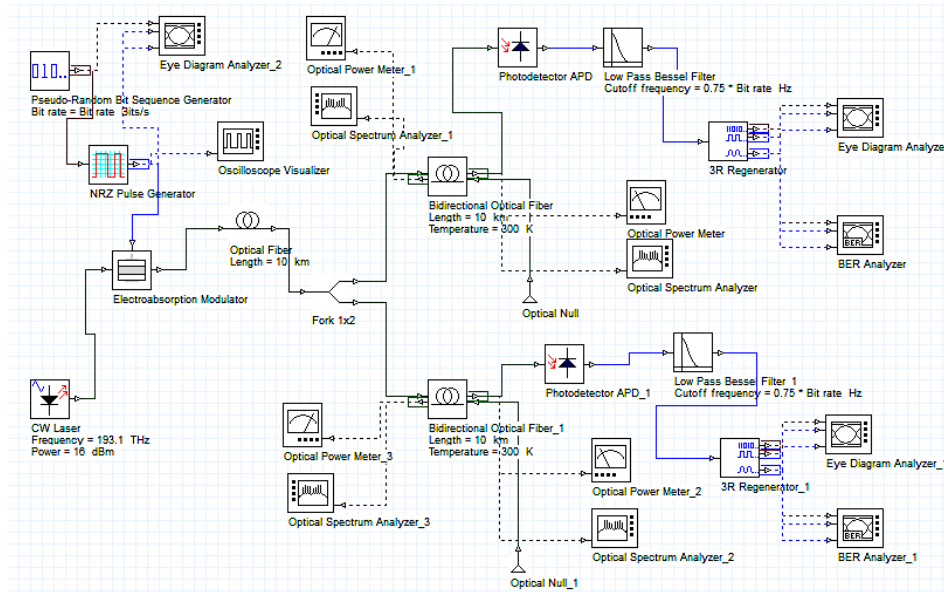


Figure 5. Multi-BOTDR remote sensing in the simulation using the Optisystem software

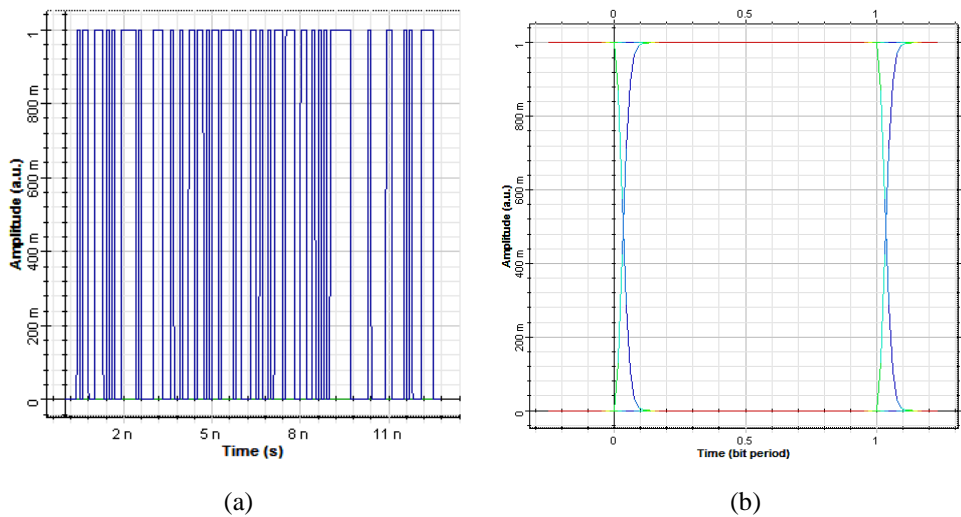


Figure 6. NRZ generated pulses (a) input signal at the transmitter and (b) eye diagram

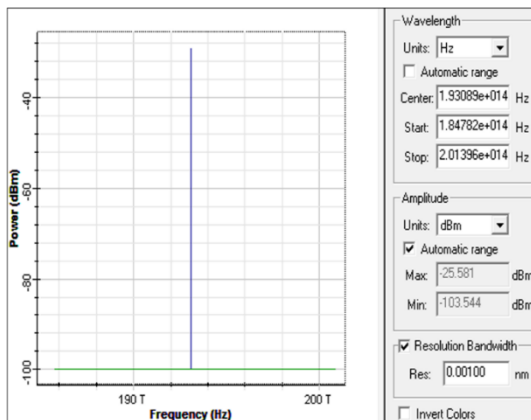


Figure 7. Backscattered frequency

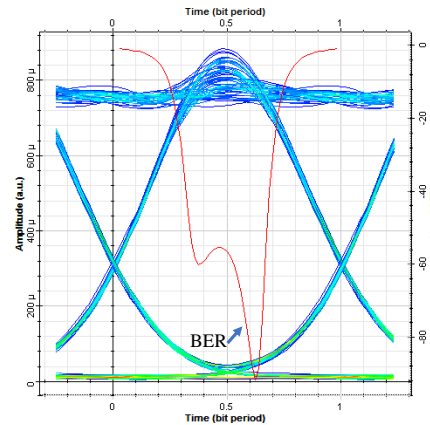


Figure 8. Eye diagram with minimum BER

Generally, the simulation design had an excellent SBS threshold power performance of 16 dB, a frequency shift of 11 GHz, and a Q-factor of 22. The developed sensor showed high SBS threshold power with 16 dB compared with 11 dB and 7.5 dB in the works of Yan and Chan [2], and Angel [4] respectively. The proposed design showed a perfect frequency shift similar to Yan and Chan [2] and equivalent to the Brillouin frequency shift. The simulation results accurately exposed the effect of Brillouin scattering on frequency shift and power level.

The backscattered power was  $-49.915$  dBm and compared with the propagated power of  $-13.034$  dBm. The backscattered power was low because the backscattered signal in a spontaneous Brillouin frequency was tremendously weak. When the backscattered power value was greater than the RBS, it was treated as the stimulated backscattered power. The SBS threshold level was defined at the crossing point between the Brillouin backscatter power as well as the RBS power, as shown in Figure 9. Consequently, the SBS threshold power should be appropriately described as the input power where the Brillouin backscatter was equivalent to the RBS at the input face.

The Brillouin power alteration coefficient was characterized as a sensing accuracy of temperature with %/K unit, where % was the percent alteration of the Brillouin backscattered power, and K was the temperature unit in Kelvin. The change in Brillouin power coefficient was observed as the sensing accuracy. It was the measured percent change of the backscattered Brillouin power affected via the variance in temperature. A high sensing accuracy was detected by a 1 K change in the temperature. A high Brillouin power change coefficient resulted in a high-power percent change amount. The backscattered power with a calculated power percent change at 300 K was applied as the reference point, as shown in Table 3. The reference point might be any chosen values as long as it was constant during the calculation of Brillouin power alteration coefficient.

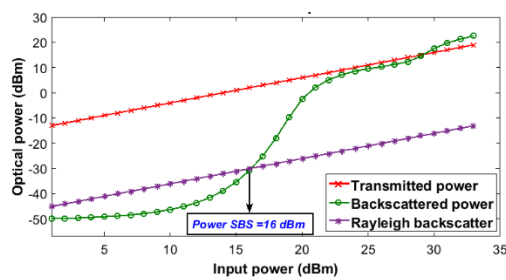


Figure 9. SBS threshold power

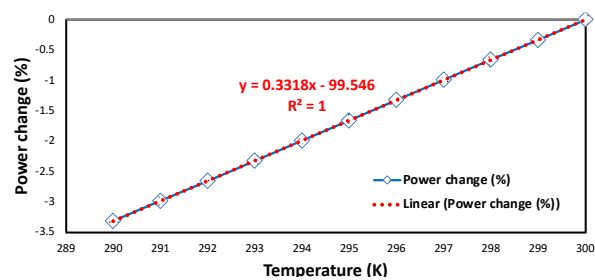


Figure 10. Calculation of Brillouin power alteration coefficient

Table 3. Calculation of power alteration (%)

Temperature (K)	Power (W; -009)	Power change (%)
290	9.859	-3.3147
291	9.893	-2.9812
292	9.926	-2.6576
293	9.960	-2.3242
294	9.994	-1.9907
295	10.028	-1.6573
296	10.062	-1.3239
297	10.096	-0.9904
298	10.130	-0.6570
299	10.163	-0.3334
300	10.197	0

The initial calculation of power alteration for a temperature of 290 K is:

$$power\ change\ (\%) = \left[ \frac{9.859 - 10.197}{10.197} \right] \times 100\% = -3.3147 \tag{9}$$

The power change was calculated for the other temperature values using (9), with  $10.197 \times 10^{-9}$  W as the reference backscattered power at 300 K. The Brillouin power change coefficient or the sensing accuracy is shown in Figure 10. (%) was the power change, and (K) was the temperature plotted in a diagram to calculate the Brillouin power change coefficient (%/K). From the slope of the appropriate line, the Brillouin power change coefficient was obtained, and the sensing accuracy was 0.3318 %/K. Overall, the developed BOTDR sensor had clear sensitivity advantages to other related sensors reported in the literature.



#### 4. CONCLUSIONS

BOTDR is a significant indicator of measuring temperature, vibration, and strain in environmental monitoring applications. In this study, remote sensing for fuel pipeline monitoring using multi-BOTDR fiber optic as a sensor platform and CW laser as the light source is designed and simulated. To sum up, multi-BOTDR fiber optic sensors utilizing Brillouin scattering are efficient considering high SBS threshold power, perfect frequency shift, and high Q-factor at a temperature operation of 300 K. The sensor is investigated for remote sensing with a wavelength of 1552.52 nm by observing the frequency shift of 11 GHz. These findings help investigate the sensing accuracy (0.3318 %/K) of the proposed sensor toward explosions, leakages, and corrosions in pipeline networks by integrating multi-BOTDR fiber optic sensors with SMF. These BOTDR sensors are characterized by a high SBS threshold, accurate sensing, and easy construction, making them a potential candidate for detecting fuel pipeline networks.

#### ACKNOWLEDGEMENTS

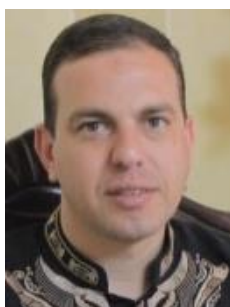
The authors would like to acknowledge Palestine Technical University–Kadoorie (PTUK) for supporting and funding this research.





#### REFERENCES

- [1] A. Shabaneh *et al.*, “Dynamic response of tapered optical multimode fiber coated with carbon nanotubes for ethanol sensing application,” *Sensors*, vol. 15, no. 5, pp. 10452-10464, 2015, doi: 10.3390/s150510452.
- [2] S. Z. Yan and L. S. Chyan, “Performance enhancement of BOTDR fiber optic sensor for oil and gas pipeline monitoring,” *Optical Fiber Technology*, vol. 16, no. 2, pp. 100-109, 2010, doi: 10.1016/j.yofte.2010.01.001.
- [3] Z. M. Hussin, M. S. Sulaiman, and P. T. Arasu, “Highly Sensitive Portable Liquid Petroleum Gas Leakage Detector,” *Journal of Telecommunication, Electronic and Computer Engineering (JTEC)*, vol. 9, no. 2-8, pp. 109-112, 2017. [Online]. Available: <https://jtec.utem.edu.my/jtec/article/view/2638>
- [4] Angel K. R., “Fiber Optic Sensing Based on Brillouin Scattering,” *International Journal of Scientific Engineering and Technology Research*, vol. 6, no. 2, pp. 0237-0240, 2017. [Online]. Available: <http://ijsetr.com/uploads/354612IJSETR13387-43.pdf>
- [5] Y. Jiang, S. Chen, C. Bi, M. Yan, and S. Jin, “Studies on backscattering noise in reflective coherent optical communication system,” *Optik*, vol. 228, p. 166169, 2021, doi: 10.1016/j.ijleo.2020.166169.
- [6] K. Inoue, “Brillouin threshold in an optical fiber with bidirectional pump lights,” *Optics communications*, vol. 120, no. 1-2, pp. 34-38, 1995, doi: 10.1016/0030-4018(95)00409-2.
- [7] M. J. Damzen, V. Vlad, A. Mocofanescu, and V. Babin, *Stimulated Brillouin scattering: fundamentals and applications*, Boca Raton: CRC Press, 2003, doi: 10.1201/9781420033465.
- [8] G. P. Agrawal, “Nonlinear fiber optics,” in *Nonlinear Science at the Dawn of the 21st Century*, Denmark: Department of Mathematical Modelling The Technical University of Denmark, 2000, pp. 195-211, doi: 10.1007/3-540-46629-0\_9
- [9] T. Shimizu, K. Nakajima, K. Shiraki, K. Ieda, and I. Sankawa, “Evaluation methods and requirements for the stimulated Brillouin scattering threshold in a single-mode fiber,” *Optical Fiber Technology*, vol. 14, no. 1, pp. 10-15, 2008, doi: 10.1016/j.yofte.2007.04.004.
- [10] H. Zhang and Z. Wu, “Performance evaluation of BOTDR-based distributed fiber optic sensors for crack monitoring,” *Structural Health Monitoring*, vol. 7, no. 2, 2008, doi: 10.1177/1475921708089745.
- [11] H. Ohno, H. Naruse, M. Kihara, and A. Shimada, “Industrial applications of the BOTDR optical fiber strain sensor,” *Optical fiber technology*, vol. 7, no. 1, pp. 45-64, 2001, doi: 10.1006/ofte.2000.0344.
- [12] Q. Li, J. Gan, Y. Wu, Z. Zhang, J. Li, and Z. Yang, “High spatial resolution BOTDR based on differential Brillouin spectrum technique,” *IEEE Photonics Technology Letters*, vol. 28, no. 14, pp. 1493-1496, 2016, doi: 10.1109/LPT.2016.2555078.
- [13] X. Feng, J. Zhou, C. Sun, X. Zhang, and F. Ansari, “Theoretical and experimental investigations into crack detection with BOTDR-distributed fiber optic sensors,” *Journal of Engineering Mechanics*, vol. 139, no. 12, 2013, doi: 10.1061/(ASCE)EM.1943-7889.0000622.
- [14] G. Fu *et al.*, “A novel positioning and temperature measurement method based on optical domain demodulation in the BOTDR system,” *Optics Communications*, vol. 480, 2021, doi: 10.1016/j.optcom.2020.126490.
- [15] R. A. Moffat, J. F. Beltran, and R. Herrera, “Applications of BOTDR fiber optics to the monitoring of underground structures,” *Geomechanics and Engineering*, vol. 9, no. 3, pp. 397-414, 2015, doi: 10.12989/gae.2015.9.3.397.
- [16] J. M. Senior and M. Y. Jamro, *Optical fiber communications: principles and practice*, England: Pearson Education, 2009. [Online]. Available: <https://shjuinpallotti.files.wordpress.com/2019/07/optical-fiber-communications-principles-and-pr.pdf>
- [17] P. Wan and J. Conradi, “Impact of double Rayleigh backscatter noise on digital and analog fiber systems,” *Journal of Lightwave Technology*, vol. 14, no. 3, pp. 288-297, 1996, doi: 10.1109/50.485585.
- [18] R. G. Smith, “Optical power handling capacity of low loss optical fibers as determined by stimulated Raman and Brillouin scattering,” *Applied optics*, vol. 11, no. 11, pp. 2489-2494, 1972, doi: 10.1364/AO.11.002489.
- [19] Maughan S. M., *Distributed fibre sensing using microwave heterodyne detection of spontaneous Brillouin backscatter*, Doctoral Thesis, Faculty of Engineering and Applied Science, University of Southampton, 2002. [Online]. Available: <https://eprints.soton.ac.uk/42382/>
- [20] A. A. Shabaneh, “Investigative Modeling of Symmetric Fiber Bragg Grating as Dispersion Compensation for Optical Transmission System,” *Optica pura y aplicada*, vol. 53, no. 4, pp. 1-13, 2020, doi: 10.7149/OPA.53.4.51052.
- [21] A. Bhardwaj and G. Soni, “Performance analysis of 20 Gbps optical transmission system using fiber Bragg grating,” *International Journal of Scientific and Research Publications*, vol. 5, no. 1, pp. 1-4, 2015. [Online]. Available: <https://www.ijsrp.org/research-paper-0115/ijsrp-p3739.pdf>
- [22] R. Kaneko *et al.*, “CW operation and performances of 1550nm-band InAs quantum-dot monolithically-integrated lasers with quantum-dot intermixed regions,” in *2020 Opto-Electronics and Communications Conference (OECC)*, 2020, pp. 1-3, doi: 10.1109/OECC48412.2020.9273725.
- [23] P. Xia, L. -H. Zhang, and Y. Lin, “Simulation Study of Dispersion Compensation in Optical Communication Systems Based on Optisystem,” *Journal of Physics: Conference Series*, vol. 1187, no. 4, 2019, doi: 10.1088/1742-6596/1187/4/042011.





- [24] G. Fu *et al.*, "A compact electro-absorption modulator based on graphene photonic crystal fiber," *Chinese Physics B*, vol. 29, no. 3, 2020, doi: 10.1088/1674-1056/ab6838.
- [25] M. M. A. Eid, A. S. Seliem, A. N. Z. Rashed, A. El-Naser, A. Mohammed, M. Y. Ali, and S. S. Abaza, "High speed pulse generators with electro-optic modulators based on different bit sequence for the digital fiber optic communication links," *Indonesian Journal of Electrical Engineering and Computer Science*, vol. 21, no. 2, pp. 957-967, 2021, doi: 10.11591/ijeecs.v21.i2.pp957-967.
- [26] O. Kharraz and D. Forsyth, "Performance comparisons between PIN and APD photodetectors for use in optical communication systems," *Optik*, vol. 124, no. 13, pp. 1493-1498, 2013, doi: 10.1016/j.ijleo.2012.04.008.

## BIOGRAPHIES OF AUTHOR



**Arafat A. A. Shabaneh**     is currently a lecturer at the Department of Communication Technology, College of Engineering and Technology, Tulkarm, Palestine. He received his BS degree from Palestine Polytechnic University, Palestine, in 2006. He completed his MS degree in communication engineering at International Islamic University Malaysia, Malaysia (2011). In 2015, he completed his Ph.D. degree at Universiti Putra Malaysia, Malaysia, in the area of optical sensors based on nanometers. He worked at the Centre of Excellence for Wireless and Photonic Network, Universiti Putra Malaysia. His research interests are optical sensors, optical communication systems, and nanotechnology. He can be contacted at email: a.shabaneh@ptuk.edu.ps.



**Raed S. M. Daraghma**     was born in 1977 in Palestine, he received his master degree from Jordan science and technology in electrical and communication engineering Jordan in 2010, and he got his P.H.D degree from Anadolu University, turkey in 2016. He has published number of papers and journals. He has engaged in educational work many years manly teaches digital communication, mobile, and digital communication networks. At Palestine technical university-kadoorie. His mainly research areas include wireless sensor network, signal processing, optical fiber communications, Narrowband internet of things. He can be contacted at email: r.daraghmeh@ptuk.edu.ps.